Loss of DJ-1 impairs antioxidant response by altered glutamine and serine metabolism

J. Meiser[1]; S. Delcambre[1]; A. Wegner[1]; C. Jäger[1]; J. Ghelfi[1]; A. Fouquier D'Herouel[1]; X. Dong[1]; D. Weindl[1]; C. Stautner[3]; Y. Nonnenmacher[1]; A. Michelucci[1]; O. Popp[10]; F. Giesert[3], S. Schildknecht[2]; L. Krämer[1]; J. G. Schneider[1,9]; D. Woitalla[7]; W. Wurst[3,4,5,6]; A. Skupin[1, 8]; D.M. Vogt Weisenhorn[3]; R. Krüger[1]; M. Leist[2]; K. Hiller[1]

[1] Luxembourg Centre for Systems Biomedicine, University of Luxembourg, L-4367 Esch-Belval, Luxembourg

[2]Doerenkamp-Zbinden Chair for In Vitro Toxicology and Biomedicine, University of Konstanz, Konstanz D-78457, Germany

[3]Helmholtz Zentrum München, German Research Center for Environmental Health, Institute of Developmental Genetics, Ingolstädter Landstr. 1, 85764 Neuherberg

[4]Deutsches Zentrum für Neurodegenerative Erkrankungen e. V. (DZNE) Standort München, Feodor-Lynen-Strasse 17, 81377 München, Germany

[5]Munich Cluster for Systems Neurology (SyNergy), Adolf-Butenandt-Institut, Ludwig-Maximilians-Universität München, Schillerstrasse 44, 80336 München, Germany

[6]Technische Universität München-Weihenstephan, Lehrstuhl für Entwicklungsgenetik, c/o Helmholtz Zentrum München, Ingolstädter Landstr. 1, 85764 Neuherberg, Germany

[7]Neurology, St. Josef Hospital, Ruhr-University, Gudrunstr. 56, 44780 Bochum, Germany

[8]National Center for Microscopy and Imaging Research, University of California San Diego, La Jolla, California, United States of America

[9]Saarland University Medical Center, Department of Internal Medicine II, Homburg/Saar, Germany

[10]Mass Spectrometry Core Facility, Max-Delbrueck Center for Molecular Medicine, Robert-Roessle Strasse 10, 13125 Berlin

Contact: University of Luxembourg, Luxembourg Centre for Systems Biomedicine
6, avenue de Swing, L-4367 Belvaux, T: +352 46 66 44 6136
karsten.hiller@uni.lu

Running Title: Loss of DJ-1 alters central metabolism

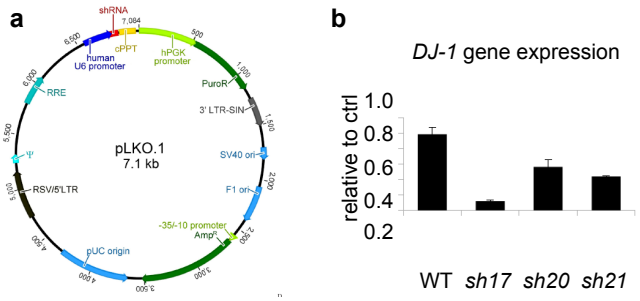

FigureS1. Related to Figure 1. DJ-1 silencing in LUHMES cells
(a) pLKO.1 was used for shRNA transfer into viral particles for subsequent transduction of proliferating LUHMES cells. (b) Tested were three different shRNA constructs (sh17, sh20 and sh21). Cells transduced with sh17, without additional clonal selection, were used for all experiments.

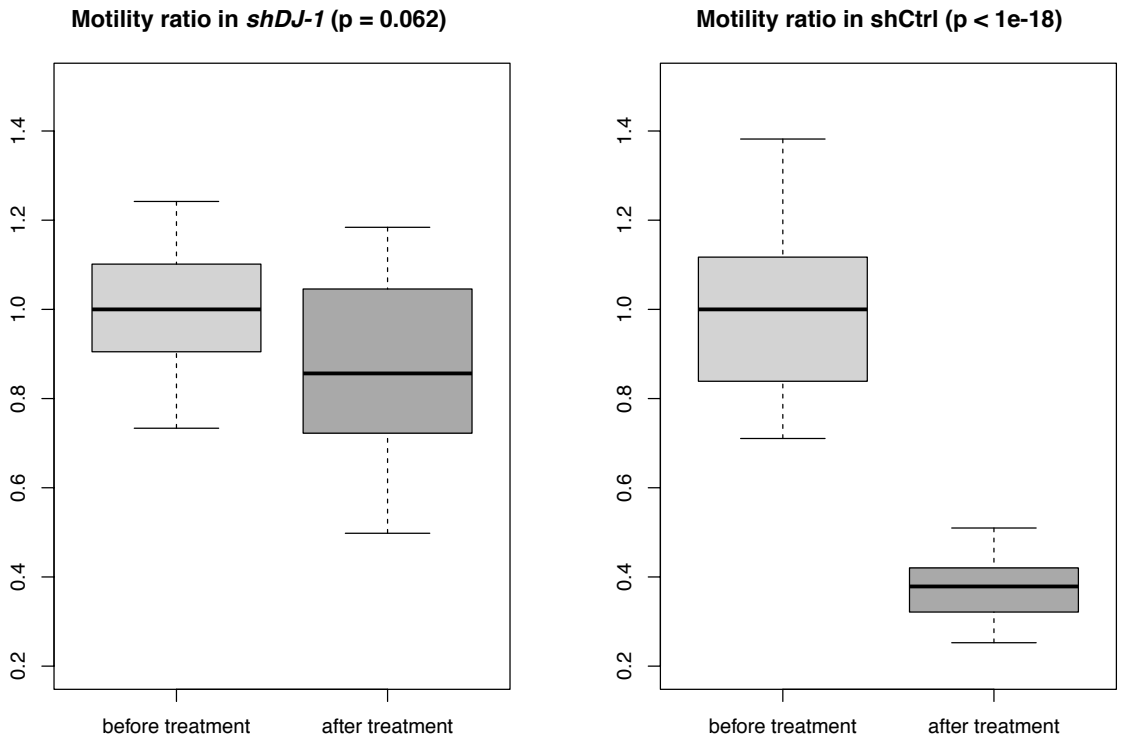

Figure S2. Related to Figure 2. Analysis of motility/stationary-ratio of TMRM stained mitochondria reveals the same effect of less deceleration in *shDJ-1* cells compared to *shCtrl*

Treatment was with 200 µM 6-OHDA after 5 minutes of imaging. Boxplots represent median values normalized to untreated control using analysis time points identical to the ones in Figure 2. (Student's t-test, number of biological replicates *n* = 3).

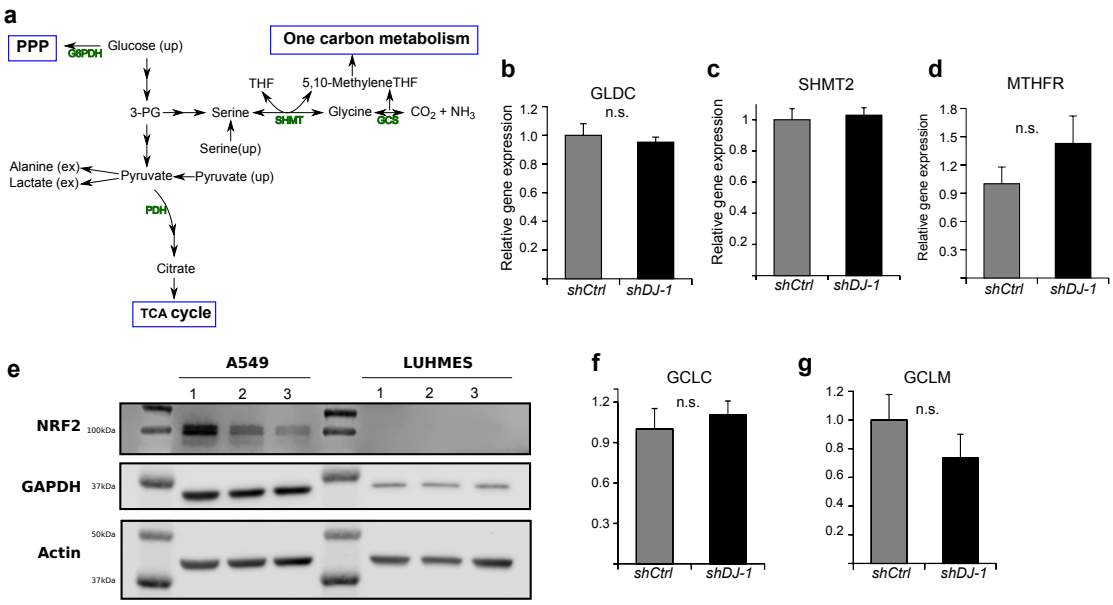

FigureS3. Related to Figure 3. Potential glucose derived carbon pathways; gene expression profiling of key enzymes that regulate these pathways and abundance of NRF2 a key regulator in antioxidant responses.

(a) Given the notion of altered glucose fluxes between *shDJ-1* and *shCtrl* cells we illustrate potential pathways in which glucose carbons can be distributed. (b-d) Gene expression of (b) glycine dehydrogenase (GLDC) (decarboxylating), (c) serine hydroxymethyltransferase 2 (SHMT2) and (d) methylene tetrahydrofolate reductase (MTHFR). (e) Western Blot against NRF2 in the lung cancer cell line A549 and LUHMES wild type cells shows no detectable protein level of NRF2 in LUHMES cells. As loading controls we used GAPDH and Actin. GAPDH is higher abundant in cancer cells compared to neurons, since cancer cells show increased glycolytic rates. 1-3 indicates three independent replicates. (f-g) Gene expression analysis of glutamate cysteine ligase, catalytic domain (GCLC) and modifier domain (GCLM) the rate-limiting enzyme of GSH synthesis. Error bars represent SEM (Welch's t-Test, $p < 0.05$; number of biological replicates: n = 3).

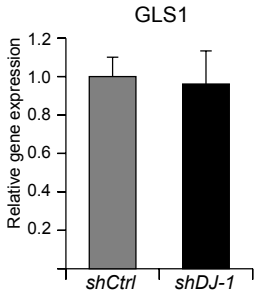

FigureS4. Related to Figure 4. Loss of DJ-1 specifically affects GLS2
Gene expression of GLS1. Error bars represent SEM (Welch's t-Test, $p < 0.05$; $n = 3$).

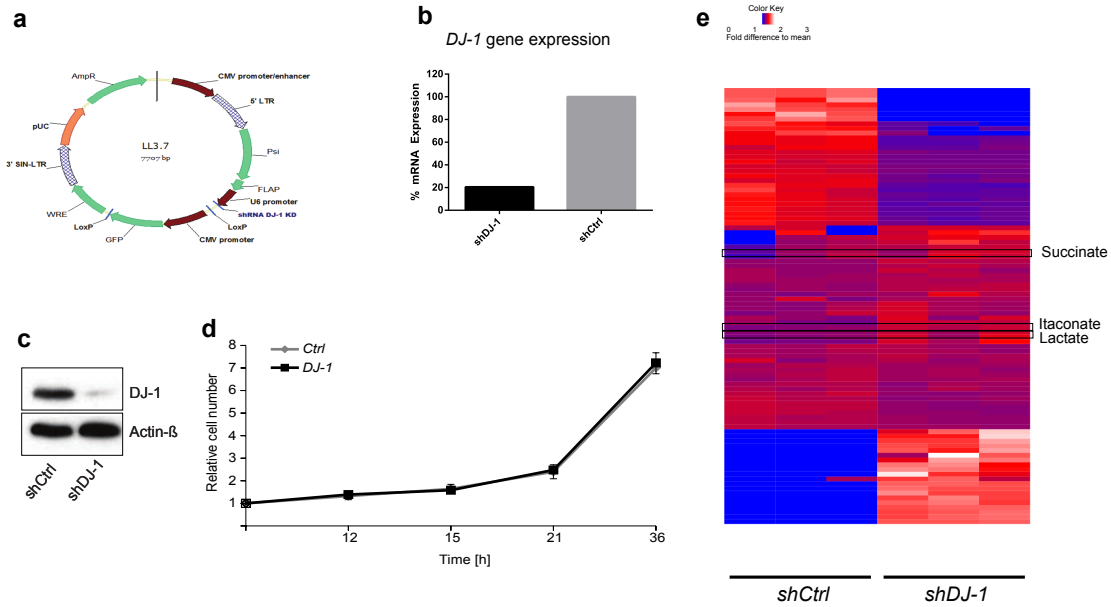

FigureS5. Related to Figure 6. DJ-1 silencing in BV-2 cells

(a) LL3.7 was used for shRNA transfer into viral particles for subsequent transduction of BV-2 cells. (b) RT-qPCR analysis showing relative mRNA abundance in shCtrl and shDJ-1. (c) Western blot analysis demonstrating DJ-1 knockdown at protein level in BV-2 shDJ-1 cells. (d) Proliferation rates of shCtrl and shDJ-1 BV-2 cells show no difference in growth. (e) Metabolome analysis of shCtrl and shDJ-1 BV-2 cells illustrated in a heatmap. Shown are significantly changed metabolites (ANOVA, $p < 0.05$; number of biological replicates: $n = 3$). Succinate, itaconate and lactate are highlighted.

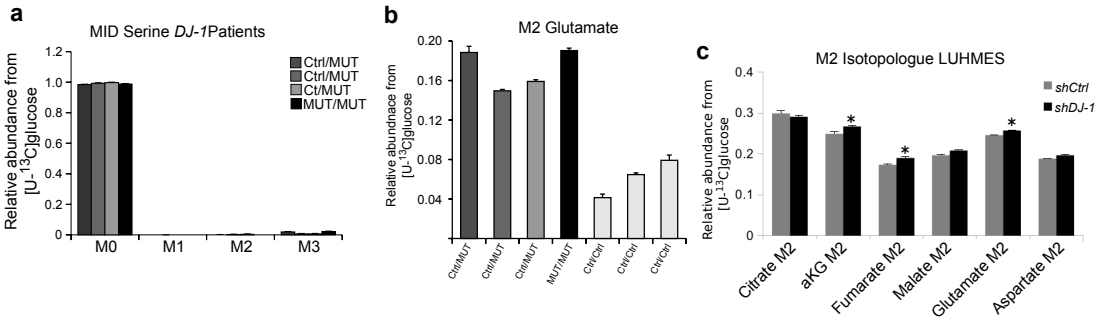

FigureS6. Related to Figure 7. Stable isotope labeling of PBMCs-derived CD14+ macrophages of DJ-1 patients carrying c.192G>C and LUHMES cells indicating decreased glutamine contribution to the TCA cycle (a) Serine biosynthesis is barely active in PBMCs derived CD14+ macrophages. (b) M2 glutamate isotopologues of patients (Ctrl/MUT: heterozygous; MUT/MUT: homozygous) and healthy controls (Ctrl/Ctrl). (c) Relative abundance of M2 citrate, M2 aKG, M2 fumarate, M2 malate, M2 glutamate and M2 aspartate in LUHMES cells using [U-^{13}C]glucose as a tracer. Error bars represent SEM. Asterisks indicate a significant difference to the respective *shCtrl*. (Welch's t-Test, $p < 0.05$; $n = 3$).